J Mater Sci: Mater Med (2010) 21:407–418
DOI 10.1007/s10856-009-3879-x

Glucuronic acid and phosphoserine act as mineralization mediators of collagen I based biomimetic substrates

Ricardo Tejero · Susanne Bierbaum · Timothy Douglas · Antje Reinstorf · Hartmut Worch · Dieter Scharnweber

Received: 5 June 2009 / Accepted: 17 September 2009 / Published online: 26 November 2009

Abstract Glucuronic acid (GlcA) and phosphoserine (pS) carrying acidic functional groups were used as model molecules for glycosaminoglycans and phosphoproteins, respectively to mimic effects of native biomolecules and influence the mineralization behaviour of collagen I. Collagen substrates modified with GlcA showed a stable interaction between GlcA and collagen fibrils. Substrates were mineralized using the electrochemically assisted deposition (ECAD) in a $Ca^{2+}/H_xPO_4^{(3-x)}$ electrolyte at physiological pH and temperature. During mineralization of collagen–GlcA matrices, crystalline hydroxyapatite (HA) formed earlier with increasing GlcA content of the collagen matrix, while the addition of pS to the electrolyte succeeded in inhibiting the transformation of preformed amorphous calcium phosphate (ACP) to HA. The lower density of the resulting mineralization and the coalesced aggregates formed at a certain pS concentration suggest an interaction between calcium and the phosphate groups of pS involving the formation of complexes. Combining GlcA-modified collagen and pS-modified electrolyte showed dose-dependent cooperative effects.

1 Introduction

Implant osseointegration depends mainly on interactions at the interface between implant surface and host tissue. Research in this field has succeeded in developing different ways to adapt implant surfaces to living tissue requirements, with a number of promising strategies based on the imitation of in vivo situations [1].

In the case of bone as a mineralized tissue, this ideally means having coatings consisting of the two main components of bone: hydroxyapatite and collagen type I [2] or, more complex, to combine calcium phosphate phases (CPP) with a type I collagen matrix in the presence of the appropriate extracellular matrix proteins [3]. Learning from the natural process of biomineralization of bone and imitating its strategies in a biomimetic approach permits the production of coatings more similar to bone both in structure and in composition [4].

In accordance with this biomimetic approach, in this work the template for mineralization consisted of collagen type I [5]. It is known that in vivo non-collagenous proteins exert a determining influence on the biomineralization of the collagen matrix via their functional groups [6, 7]. Such functional groups are therefore of interest also in an artificial extracellular matrix (ECM) [8]. Glycoproteins such as bone sialoprotein (BSP) [9, 10] or osteopontin (OPN) [11], and proteoglycans (PGs) such as decorin or biglycan, [3, 12–14] interact with calcium phosphates due to their high amounts of acidic aspartic and glutamic residues or phosphorylated aminoacids, and thus influence mineralization.

For collagen–hydroxyapatite biomaterials with more bone-like characteristics, simplified strategies using model molecules able to mimic these typical functions of native extracellular matrix components may therefore be of interest. Thus, based on decorin and osteopontin, respectively, the simple functionalities glucuronic acid (GlcA) and phosphoserine (pS) were chosen for this study.

Decorin is a small leucine-rich proteoglycan, which associates with collagen fibrils and is known to intervene directly in the control of matrix organization [15, 16].

R. Tejero (✉) · S. Bierbaum · T. Douglas · A. Reinstorf · H. Worch · D. Scharnweber
Max Bergmann Center of Biomaterials, Dresden University of Technology, Budapester Str. 27, 01069 Dresden, Germany
e-mail: ricardo@minin.es

It is composed of repeating disaccharide units of GlcA and *N*-acetylgalactosamine. These monosaccharides are released as a product of the enzymatic degradation of some glycosaminoglycan (GAG) chains during deglycosylation, a process that has been detected as an intermediary step during the in vivo mineralization of bone [17]. Paschalakis et al. [12, 14] suggested that, compared to decorin, monomers such as GlcA could bring about an enhanced rate of HA nucleation. The GlcA acidic groups seem to be able to bind not only to inorganic compounds but also to organic molecules like various ECM proteins, growth factors and cell surface receptors [18].

Assuming that GlcA binds to collagen in a process of non-enzymatic glycosylation between collagen amino groups and GlcA's anomeric centre [19], it seems possible that GlcA will increase the electrostatic binding of Ca^{2+} to the protein structure through its free carboxylate group, acting thus as a template for biomineralization in the organic matrix. The use of GlcA alone in this study may allow distinguishing its effect from the wide range of crystal growth regulatory functions observed in greater PG aggregates, as for example, the role of their sulphatation pattern or the conformation of GlcA in the chain, which has been reported to dictate its role as promoter or inhibitor of mineralization [20, 21].

Osteopontin (OPN) and bone sialoprotein (BSP) are non-collagenous phosphoproteins proven to play a role in the mineralization of bone. Both contain high amounts of phosphorylated residues which are partly responsible for their Ca^{2+} binding capability, and thus for their control of crystal growth [9–11, 17]. Based on this fact phosphoserine, a phosphorylated amino acid can be assumed to be a successful model molecule [22–24]. It should be expected that the presence of pS in solution would emulate the inhibitory effect of OPN reported by Hunter et al. [11].

The use of a biomimetic approach also requires methods of mineralization capable of imitating in vivo conditions and enabling the model molecules to play the desired role. Many methods have been developed to produce bioactive calcium phosphate coated surfaces [25]. We chose the method of electrochemically assisted deposition (ECAD) of calcium phosphate phases (CPP) because it allows the formation of thin CPP coatings within a short time and under very reproducible and defined conditions [26], even in the case of surfaces functionalized with an adsorbed organic matrix [8]. The fine control of the alkalinization level at the surface of the metallic substrate is one of the main advantages of the ECAD method, because it achieves the formation of hydroxyapatite (HA) through a dissolution–redeposition process of ACP, which is highly dependent on pH [26]. Increase of the current density or deposition time leads to crystalline HA [27].

This work aims at analyzing the influence of mediators on the mineralization of collagen type I based biomimetic substrates. Glucuronic acid (bound to collagen) and phosphoserine (present in the electrolyte) are used as model substances for proteoglycan deglycosylation products and for phosphoproteins, respectively. With respect to biomaterial applications aiming at improving the osseointegration of implants, the mineralization is performed with collagenous substrates immobilized on titanium surfaces. Our results provide the first quantitative characterization of the interaction of GlcA with collagen type I with respect to fibrillogenesis and mineralization behavior. Additionally, we have analyzed the influence of pS present in the electrolyte during deposition of calcium phosphate phases for collagen substrates with and without bound GlcA. By adding pS at this point, we expected to block the incorporation of mineral ions into the surface, which may give rise to the inhibition of the crystal growth as well as changes in the properties and morphology of the existing crystal.

2 Materials and methods

2.1 Materials

Unless otherwise stated, the chemicals used in this work were of high purity (A.C.S. reagent grade) and provided by Sigma–Aldrich Chemie GmbH Germany. The collagen employed was acid soluble calfskin collagen type I from Fluka, Sigma brand, Prod. No. 27664.

Discs of titanium alloy Ti6Al4V (ASTM136, 10 mm diameter and 2 mm thickness) were ground and polished using a titanium oxide suspension (anatase, particle size: 20 nm). Smooth surfaces were used in order to avoid surface-induced nucleation. They were cleaned with 1% Triton X-100, acetone, and 96% ethanol, rinsed with distilled water, and air-dried.

2.2 Preparation of samples for mineralization

Collagen was dissolved in 10 mM CH_3COOH overnight at 4°C at a concentration of 2 mg/ml. The resulting collagen solution was mixed with equal volumes of buffer consisting of 30 mM phosphate at pH 7.4 on ice. Fibrillogenesis was started by raising the temperature to 37°C and allowed to take place for 18 h at this temperature. When GlcA was included, it was dissolved in the buffer at a concentration of 1 mg/ml and added prior to the start of fibrillogenesis to concentrations of 50, 250 and 500 μg/ml.

The resulting fibrils were centrifuged for 15 min at 10,000×*g* to separate the fibrils (pellet) from remaining

collagen monomers and small oligomeric aggregates. The collagen not integrated into fibrils was determined in the supernatant using the method of Lowry et al. [28], and the amount of fibrillar collagen was calculated from this data. The pellet was accordingly resuspended to a concentration of 1 mg/ml in the phosphate buffer and homogenized (Ultra-Turrax, IKA Labortechnik).

Titanium samples were coated with 100 µl collagen solution and after 10 min air drying, rinsed with distilled water.

2.3 Electrochemically assisted deposition

For electrochemically assisted deposition a combined potentiostat/galvanostat (PJT 120-1 Radiometer) was coupled with a double-wall electrochemical cell that ensured constant temperature (36 ± 1°C) during electrolysis. The working electrode was switched cathodic and the polarization was performed in galvanostatic mode. For experiments, current density ranged from −0.76 to −9.76 mA/cm^2. The polarization time varied between 1 and 60 min. The electrolyte used for deposition of CPPs was prepared with concentrations of 1.66 mM $CaCl_2$ and 1 mM $NH_4H_2PO_4$ (both Fluka, Neu-Ulm, analytical grade). For the deposition electrolyte containing pS, crystalline *O*-phospho-L-serine (Fluka) dissolved in distilled water at a concentration of 1 mg/ml and was added to the electrolyte at molar pS/Ca ratios ranging from 1:2000 to 1:20. The final pH of the electrolyte was adjusted to 6.4 with ammonium hydroxide solution (Merck). The coatings were rinsed five times with distilled water and allowed to dry in air at room temperature for at least 2 h.

2.4 Characterization of surface morphology

Scanning Electron Microscopy (SEM) was performed using a DSM 982 Gemini, Carl Zeiss. Samples were carbon-coated to improve surface conductivity. Best definition was obtained at acceleration voltages of 1 and 2 kV. In order to characterize the nanometer scale structure of the collagen fibrils, Atomic Force Microscopy (AFM), Bioscope; Digital Instruments/Veeco, using tapping mode was performed.

2.5 Analysis of CPP

Fourier Transform Infrared Spectroscopy (FTIR, Perkin-Elmer FTS2000, with microscope unit) was used to analyze the phase composition of the deposited CPP. At least three scans per spectra and five spectra from each distinct surface state in different positions of each sample were taken to check homogeneity.

2.6 GlcA quantification

GlcA quantification was performed according to a modified version of the method described by Mecozzi [29]. Briefly, collagen fibrils were resuspended in 1 M CH_3COOH (1 ml ± 0.05) and sonicated for 4 h at room temperature (Bandelin Sonorex TK52, HF = 35 kHz). 1 ml of each sample was mixed with 0.5 ml 5% Phenol and 2.5 ml 95–98% H_2SO_4 in glass flasks and incubated at room temperature for 30 min prior to measuring absorption at 485 nm (SpectraFluorPlus, TECAN).

2.7 GlcA desorption

For desorption experiments, collagen fibrils were resuspended in 1 M NaCl immediately after fibrillogenesis and incubated for 2 days at 37°C. The supernatant and the pellet were separated and each mixed with 1 ml 1 M CH_3COOH. GlcA content was determined as described above.

2.8 Statistics

For analysis of statistical significance experiments were repeated at least three times. Mean values ± standard deviation were calculated for each concentration of GlcA studied. Results for collagen fibril formation and GlcA content of fibrils were analyzed by one-way ANOVA (analysis of variance). $P < 0.05$ was considered statistically significant.

3 Results

3.1 Influence of GlcA on collagen fibril formation and morphology

Influence of GlcA concentration on the amount of collagen fibrils formed during fibrillogenesis is summarized in Fig. 1. While the integration of collagen into fibrils is in the range of 75% with no GlcA present, a monotonous decrease of the amount incorporated is detected with rising GlcA concentrations, with the integration decreasing to about 50% for the highest GlcA concentration used.

3.2 Integration and desorption of GlcA

The results of the GlcA quantification experiment are displayed in Fig. 2. The boxes give the amount of GlcA detected in collagen after fibrillogenesis as a function of the GlcA concentration added to the collagen solution prior to fibril formation. The amount of GlcA bound is related to the amount present during fibrillogenesis, though the

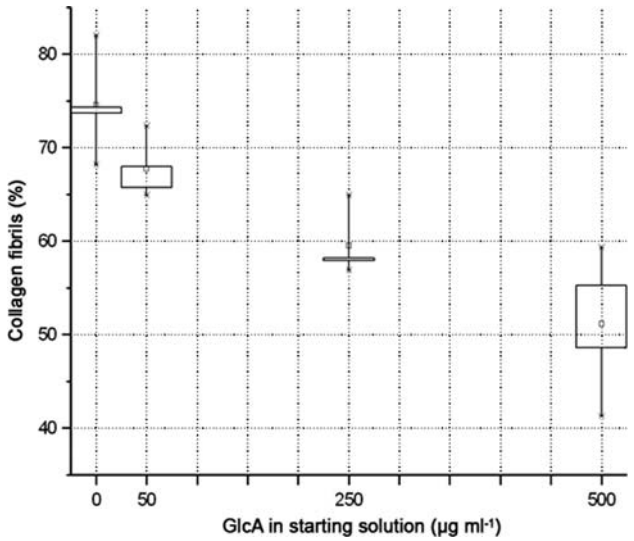

Fig. 1 Box plot of the extent of collagen monomer integration into fibrils in % as a function of the concentration of GlcA added to the initial collagen solution in µg ml^{-1}

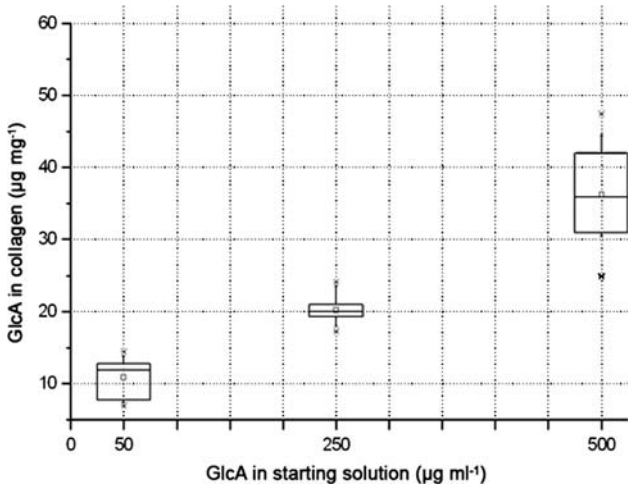

Fig. 2 Box plot of the amount of GlcA bound in µg per mg fibrillar collagen as a function of the concentration of GlcA added to the initial collagen solution in µg ml^{-1}

relation is not linear. For low concentrations of GlcA a proportionally higher amount is bound, such as about 11 µg GlcA per mg collagen for a concentration of 50 µg/ml GlcA. A five fold higher GlcA concentration of 250 µg/ml in the initial fibrillogenesis solution is necessary in order to increase the bound amount by a factor of two. However, for all experimental conditions the GlcA content of the fibrils is below 4% of the total fibril mass.

Only negligible amounts of GlcA were found to desorb over a period of 2 days in a 1 M NaCl solution at room temperature, irrespective of the GlcA concentrations used in the fibril formation process. The results of these experiments are shown in Fig. 3.

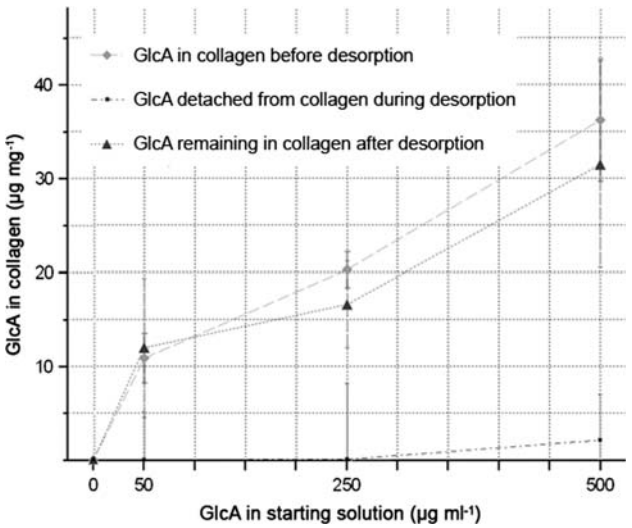

Fig. 3 Amount of GlcA bound in µg per mg fibrillar collagen before and after desorption in 1 M NaCl as a function the concentration of GlcA added to the initial collagen solution. Line through data is a guide to the eye

3.3 Influence of the GlcA content on fibrils morphology

In Fig. 4, AFM micrographs show no distinct alteration of the fibrils banding pattern or thickness when formed in presence of GlcA.

3.4 Influence of the GlcA content of fibrils on mineralization

The collagen fibrils adsorbed on titanium discs were subjected to cathodic polarization in a galvanostatic regime with current densities ranging from −0.76 to −9.76 mA/cm^2 and polarization times from 5 and 15 min. The coatings obtained were evaluated through infrared spectroscopy to analyze the phase composition of the deposited CPP and scanning electron microscopy to assess their morphology. Table 1 correlates phases to the experimental conditions for each coating. Regarding unmodified and GlcA-modified collagen matrices, CPPs could be classified as either non-apatitic CPPs (ACP) or highly-ordered nanocrystalline carbonated hydroxyapatite (HA). Some samples showed presence of both phases, depending on the scan region. As differences between samples and scans where mainly related to peak intensities and hydration level, two representative spectra of the phases encountered were retained and are shown in Fig. 5.

Irrespective of the substrate GlcA content and the applied current density, after 5 min of cathodic polarization—the shortest time studied—the resultant coatings gave spectra with broad single bands around 570 cm^{-1} and 1028 cm^{-1}, ascribed to phosphate v_4 and v_3 absorption

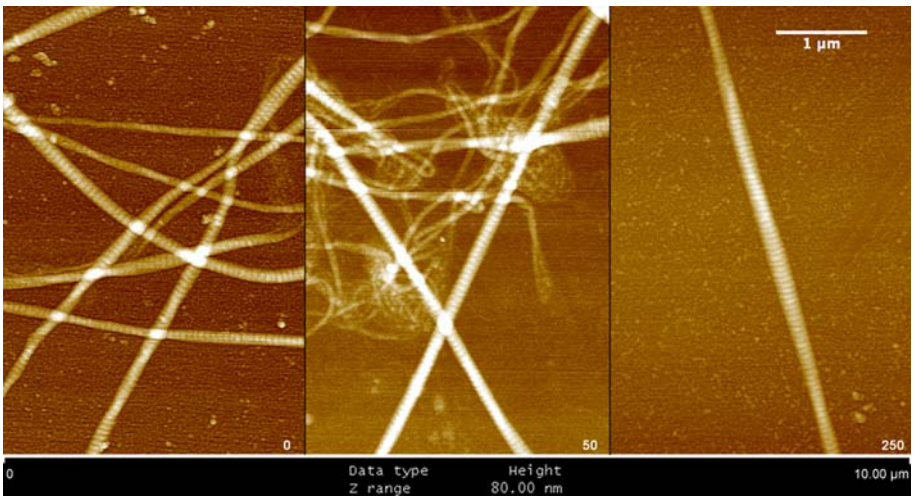

Fig. 4 AFM height micrographs of collagen fibrils unmodified and modified with 50 and 250 µg ml^{-1} GlcA. No significant modification of the banding pattern and diameter caused by the presence of GlcA is observed

Table 1 Summary of experimental conditions and coatings obtained

ECAD conditions		Role of model molecules		Calcium Phosphate Phases	
Current density (mA/cm^2)	Time (min)	GlcA in collagen (µg/ml)	Electrolyte pS/Ca^{2+}	FTIR	SEM
−0.76 to −9.76	5; 15[a]	0–500	0	ACP (Fig. 5)	Sparse coating of spherical nanoparticles (Fig. 6)
−7.64; −9.76	15	0; 50			Dense coating of spherical nanoparticles (Fig. 8a)
		250		ACP/HA (Figs. 5, 7)	Mixed coating of spherical nanoparticles and needles (Fig. 8b)
		500		HA (Fig. 5)	Dense coating of needles (Fig. 8c)
−9.76		0–500	1:40; 1:20	ACP (Fig. 9a)	Dense coating of spherical nanoparticles (Fig. 8f)
	20; 30	0	0	HA (Fig. 9b1, c1)	Dense coating of needles (Fig. 8d, g)
	20		1:40	Non-apatitic (Fig. 9b3)/HA (Fig. 9b2)	Agglomerated coating with distinguishable nanoparticles (Fig. 8e)
	30	0–500		Non-apatitic (Fig. 9b4, c2, c3)	Agglomerated coating (Fig. 8h, i)
	20; 30	0	1:20		

[a] Only for 0,76 mA/cm^2

modes, respectively and typical for non-apatitic disordered domains. SEM observations showed a shallow coating of spherical nanoparticles of diameters ranging between 50 and 150 nm (Fig. 6).

This was also the case for all substrates polarized at the lowest current density of −0.76 mA/cm^2 irrespective of the polarization time, whereas for higher current densities, the amount of GlcA in the fibrils affected the mineralization behavior of the substrates.

For a polarization time of 15 min and current densities of −7,64 mA/cm^2 and −9,76 mA/cm^2, GlcA concentrations below 250 µg/ml in the fibrillogenesis solution (around 20 µg GlcA per mg of collagen fibril) yielded coatings densely populated with spherical nanoparticles (Fig. 8a). FTIR spectroscopy determined again the non-apatitic nature of the coating (Fig. 5).

However, for 250 µg/ml (∼20 µg/mg) GlcA concentration, two different types of spectra were detected depending on the scan region. The first kind of spectra corresponded to the mentioned disordered domains, but here the v_4 phosphate region showed an incipient splitting of the 570 cm^{-1} band (Fig. 7). The second kind of spectra corresponded to the domains also found for 500 µg/ml (∼36 µg/mg) GlcA concentrations (see below), but peaks were less faint. SEM images showed a mixed morphology consisting in spherical nanoparticles with interspersed acicular needles (Fig. 8b).

Keeping this latter ECAD parameters, spectra corresponding to 500 µg/ml GlcA (∼36 µg/mg) showed clearly the characteristic splitting between the v_3 phosphate absorption band (1028, 1090 cm^{-1}) and the triply degenerated v_4 phosphate-bending mode of the P–O–P bond at

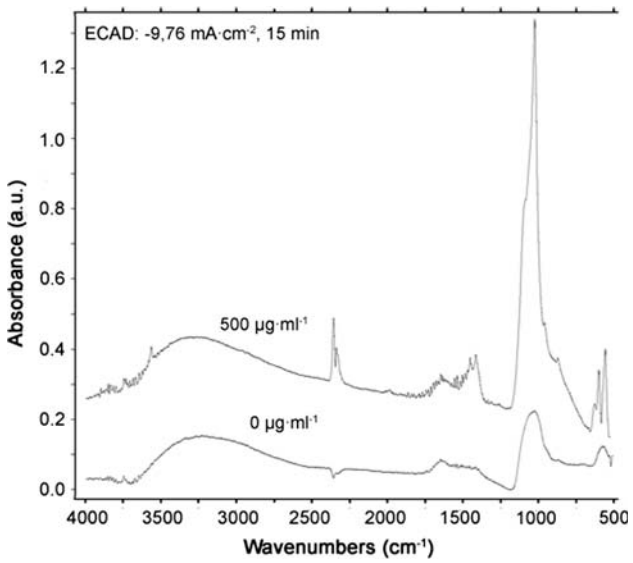

Fig. 5 FTIR spectra of calcium phosphate phases deposited by ECAD at -9.76 mA cm^{-2} for 15 min on unmodified and 500 µg ml^{-1} GlcA-modified collageneous substrates

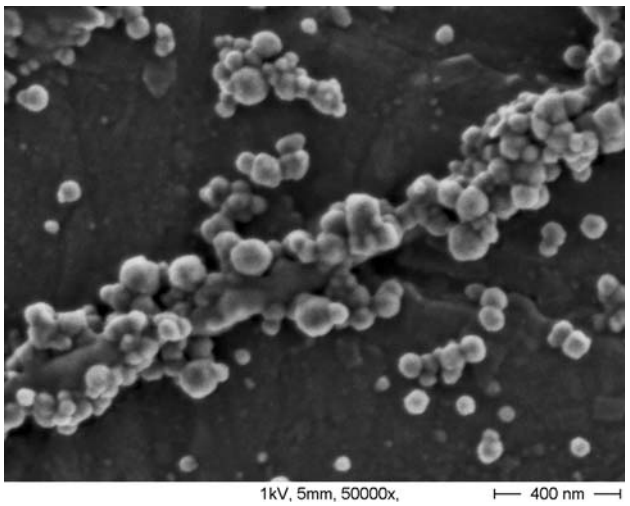

Fig. 6 SEM micrograph of calcium phosphate phases deposited by ECAD on collageneous substrates modified with 500 µg ml^{-1} GlcA. ECAD at $-0{,}76$ mA cm^{-2} for 5 min

561 cm^{-1}, 575 cm^{-1} (shoulder) and 603 cm^{-1}, typical for nanocrystalline apatites [30]. The hydroxyl librational mode at 632 cm^{-1} could also be seen as well as the v_1 phosphate peak at 963 cm^{-1}. Bands assigned to carbonate were also detected (bending v_2 at 875 cm^{-1}, stretching v_3 at 1418 cm^{-1}, and bending v_{3-4} at 1456 cm^{-1}) [31]. The hydroxyl stretching vibration at 3567 cm^{-1} was also distinguishable (Fig. 5). The morphology of the coatings was consistent with the phase compositional findings and corresponded to a dense coating of needle-like nanocrystals (Fig. 8c).

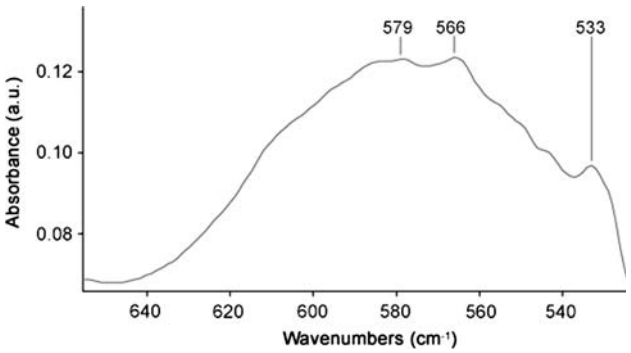

Fig. 7 FTIR spectrum of the v_4 phosphate domain of calcium phosphate phases deposited by ECAD at -7.64 and -9.76 mA cm^{-2} for 15 min on 250 µg ml^{-1} GlcA-modified collageneous substrates

3.5 Influence of the GlcA content of fibrils on mineralization

The adsorbed substrates were subjected to cathodic polarization in a galvanostatic regime at -9.76 mA/cm^2 for 15, 20 and 30 min in electrolytes containing pS concentrations from 0.152 µg/ml to 15.2 µg/ml, which corresponds to pS/Ca^{2+} molar ratios ranging from 1:2000 to 1:20.

Samples polarized for 15 min in an electrolyte containing pS/Ca^{2+} ratios of 1:40 and 1:20 did not differ noticeably from the reference without pS. Their FTIR spectra showed a general decrease in peak intensities and absence of the ACP broad band around 570 cm^{-1} as compared to the reference (Fig. 9a). In the case of the 1:40 sample, the peak at 875 cm^{-1} as well as the broadening around 1418 cm^{-1} of carbonate was no longer detected (Fig. 9a2).

After 20 min of deposition, IR spectroscopy on the reference sample indicated well crystallized HA (Fig. 9b1). This spectrum is also detected in the case of 1:40 pS/Ca^{2+} samples, but not for all regions scanned (Fig. 9b2). Regions corresponding to non-apatitic material of low peak intensity were equally detected (Fig. 9b3). Albeit the absence of peak splitting around 1050 cm^{-1}, the broad band around 570 cm^{-1}, typical for the disordered state, seems shifted to a lower wavelength around 532 cm^{-1} [32]. In the case of 1:20 pS/Ca^{2+}, all samples produced spectra of a slightly different form (Fig. 9b3). Incipient splitting is seen around 1050 cm^{-1} (peak at 1023 cm^{-1} and shoulder at 1090 cm^{-1}) but unclear information is retrieved in the v_2 phosphate domain (560–605 cm^{-1}). Again a peak at 532 cm^{-1} is detected.

SEM images of the samples are shown in (Fig. 8). In the case of samples polarized for 15 min, the aspect of the surface was similar, for all pS concentrations studied (Fig. 8a). This situation changed for polarization times of 20 min. Whereas in the case of the reference (without pS

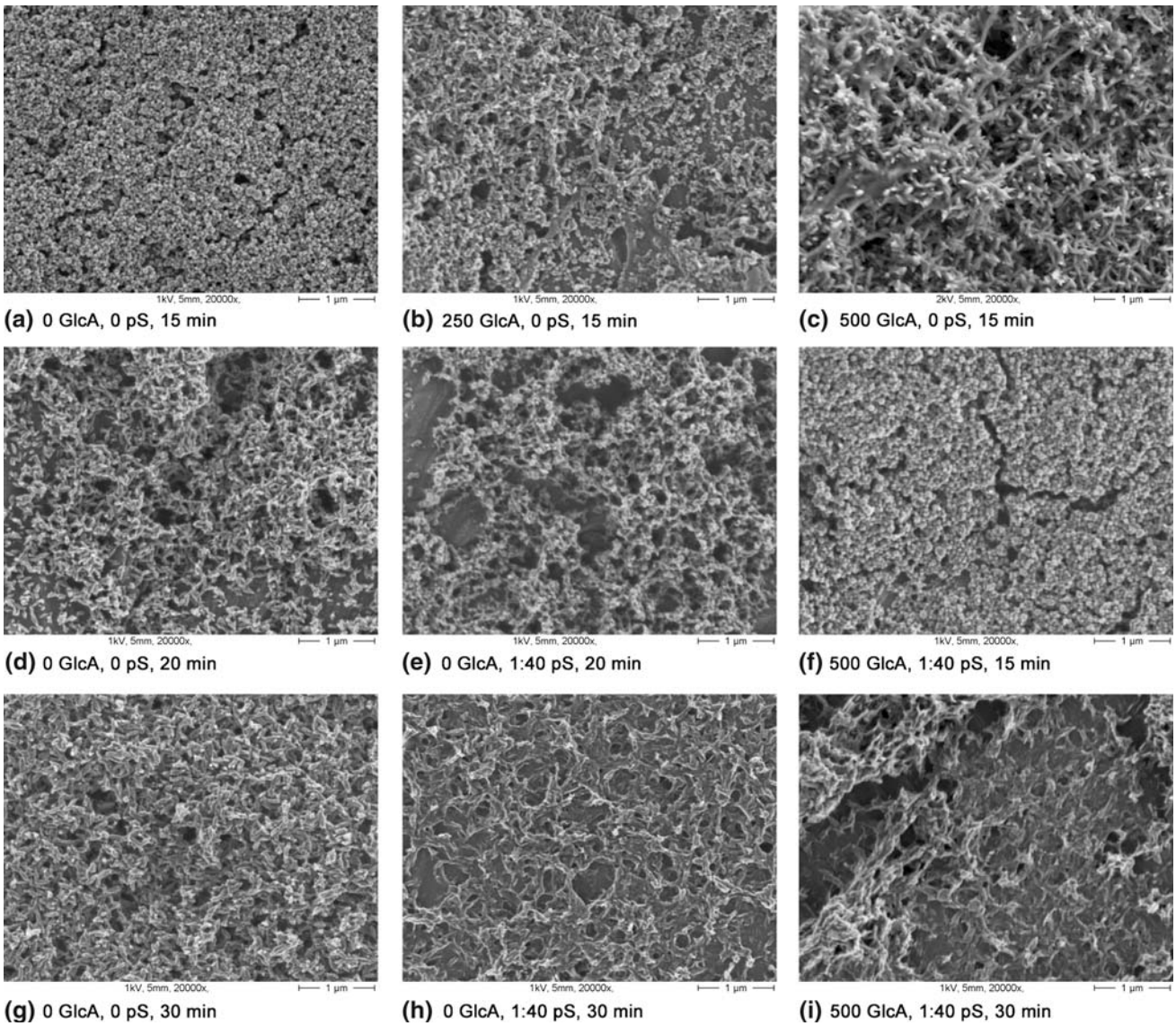

Fig. 8 SEM micrographs of calcium phosphate phases deposited by ECAD at -9.76 mA cm^{-2} for 15 min (**a**, **b**, **c**, **f**), 20 min (**d**, **e**) and 30 min (**g**, **h**, **i**) on collageneous substrates unmodified (**a**, **d**, **e**, **g**, **h**) and modified with 250 μg ml^{-1} GlcA (**b**) and 500 μg ml^{-1} GlcA (**c**, **f**, **i**) in the presence of electrolytes unmodified (**a**, **b**, **c**, **d**, **g**) or modified with 1:40 pS/Ca^{2+} ratio (**e**, **f**, **h**, **i**)

Fig. 8d), the coating consists mainly of HA, a mixture of coalesced agglomerate of ACP/HA forms in the presence of pS (Fig. 8e).

After 30 min of polarization at -9.76 mA/cm^2, the reference sample shows a layer of distinct HA crystals (Fig. 8g). However the crystals formed with 1:40 pS/Ca^{2+} in the electrolyte are again agglomerated (Fig. 8h) and its spectrum is close to the one found for 20 min.

Comparing the intensities of the different spectra analyzed indicate that for all the polarization times applied the amount of CPP detected decreases with increasing pS concentration in the electrolyte. This was further confirmed by the exhaustive mapping of the samples through SEM (data not shown).

3.6 Joint influence of GlcA content of fibrils and pS in the electrolyte on mineralization

Collagen fibrils without GlcA and formed with 250 and 500 μg/ml GlcA during fibrillogenesis respectively, were polarized with a current density of -9.76 mA/cm^2 for 15 and 30 min in electrolytes with pS/Ca^{2+} molar ratios between 0 and 1:20. In Fig. 8 SEM images are shown only for the ratio 1:40, because the ratio of 1:1000 pS did not noticeably influence the mineralization behaviour and the results at ratio of 1:20 were close to that at the lower one of 1:40.

After 15 min of ECAD, collagen without integrated GlcA, displayed a uniform coating of ACP spheres independent of the pS content of the electrolyte (Figs. 5, 8a).

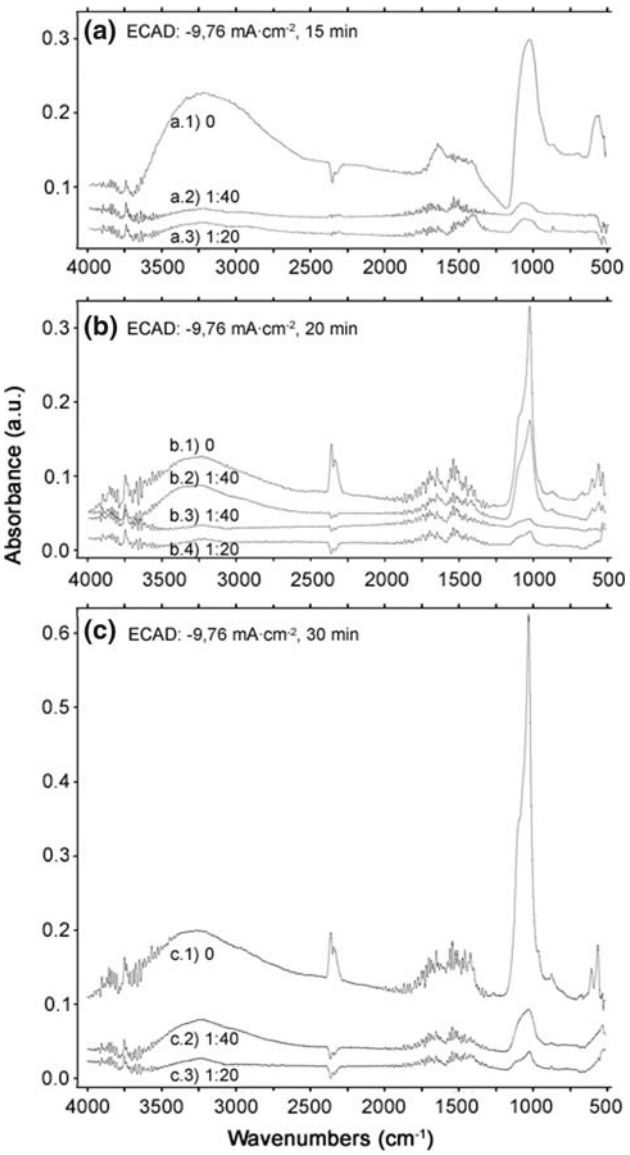

Fig. 9 FTIR spectra of calcium phosphate phases deposited by ECAD at -9.76 mA cm^{-2} for **a** 15, **b** 20 and **c** 30 min on collageneous substrates. Electrolyte unmodified or modified with 1:40 and 1:20 pS/Ca^{2+}

In the case of collagen fibrils prepared with 500 μg/ml GlcA present during fibrillogenesis (~36 μg/mg), mineralization without pS gave rise to HA coatings (Figs. 5, 8c). For a pS/Ca^{2+} concentration of 1:40, though, the coatings consisted completely of ACP spheres (Fig. 8f). This was also the surface state found when collagen was modified with 250 μg/ml GlcA (~20 μg/mg) for substrates generated in the presence of 1:40 pS, whereas in the absence of pS, mineralization yielded a surface of HA crystals mixed with ACP (Figs. 5, 8b). FTIR spectra of both types of mineralized substrates (250 and 500 μg/ml GlcA concentrations) issued of pS-modified electrolytes were similar to the ACP spectra shown in Fig. 5.

After 30 min of polarization with electrolytes containing 1:40 pS and 500 μg/ml GlcA modified collagen substrates, neither the spectra nor the morphology of the resulting coatings differed with respect to the samples without GlcA (morphology of Fig. 8i and spectra of Fig. 9c2).

4 Discussion

The present study investigates the mineralization behavior of collagenous substrates in combination with model molecules based on such components of the native extracellular matrix as are expected to play a major role in the in vivo biomineralization. GlcA as a representative of the class of the glycosaminoglycans was immobilized in collagen fibrils adsorbed to titanium samples as a model for implant surfaces and electrochemically assisted mineralized in the presence and absence of pS as a model for the acidic functionality of phosphoproteins.

4.1 Interaction of GlcA with collagen type I

The inclusion of GlcA in the process of fibrillogenesis does not noticeably affect fibril morphology for all concentrations studied, though the integration of collagen monomers into fibrils is somewhat reduced if high amounts of GlcA are present during fibrillogenesis (Fig. 1). However the characteristic banding pattern indicates that the typical quarter staggered association of the collagen monomers could still take place. The decrease in the incorporation of tropocollagen into fibrils has also been reported to happen for fibrillogenesis in the presence of decorin monomers [21, 33]. This reduction in monomer integration might be due to a slight steric hindrance due to the already bound GlcA and contributed by the formation of GlcA–collagen monomer aggregates in solution, which would not allow fibrils to form.

The amount of GlcA bound is related to the amount present during fibrillogenesis, but the relation is not linear. Though this is indicative of a saturation of GlcA binding, detailed experiments with higher GlcA concentrations are needed to establish if and where a plateau region exists.

The bound GlcA did not desorb in 1 M NaCl solution, which indicates that the interaction between GlcA and collagen is not based primarily on ionic interactions. A possible reaction pathway between GlcA and collagen would consist in the formation of an imine base as a result of the interaction of the anomeric carbon of the open chain of GlcA with the amino groups of lysine residues followed by slow spontaneous Amadori rearrangement to a more stable 1-amino-1-deoxyketose structure.

This explanation is consistent with the findings of Ding et al. [19], who detected major binding sites for GlcA at

lysine Lys-195, -199 and 525 and minor at Lys-137, 351 and -541. Furthermore Lys-525 was identified as the primary site for non-enzymatic glycation, with Lys-351 also involved at some extent. [19, 33–35].

In regard of the tendency shown in Fig. 2 and the progressive decrease of lysine binding site availability, the existence of a saturation limit beyond which no more GlcA could be bound by the fibrillating collagen is expected.

4.2 Mineralization behaviour of GlcA–collagen substrates

Regarding the GlcA influence on mineralization, the results show that the GlcA-modified substrates perform a dose-dependent shift to the thermodynamically more stable mineral HA before unmodified matrices do. This may be due to the fact that GlcA acts as a nucleating agent for HA when combined to collagen. The binding model proposed above implies that collagen-bound GlcA may expose one free carboxylate functionality per molecule, which in turn would be able to attract and bind Ca^{2+} by electrostatic interactions. Accordingly, the introduction of GlcA into the collagenous matrix would increase the number of negative charges driving to a higher Ca^{2+} surface concentration, suggesting the creation of a higher amount of nucleation sites on the surface of the collagen fibrils, though this has yet to be confirmed by high-resolution images of lightly mineralized matrices using AFM or TEM.

The early-formed CPPs have been identified as Amorphous Calcium Phosphate (ACP) in agreement with former work both in our group [26, 27, 36] and in other groups [37]. The phase transformation to form apatite crystals starts with initial spheres consisting of $Ca_3(PO_4)_2{\cdot}nH_2O$ from which crystalline HA needles grow. The process would proceed step-wise, taking advantage of a meta-stable disordered and more soluble stage with lower activation energy to overcome the higher activation barrier needed for the formation of the less soluble and ordered HA. This transient precursor strategy has been used to explain the mechanisms of formation not only of synthetic apatites [26, 27] but also of apatites of biological nature, be it based on ACP or OctaCalcium Phosphate (OCP) precursors [37–39]. Recent investigations claim also evidence of OCP and ACP as transient precursor for biological apatite [40–42]. However, the detection of non-apatitic phosphates as a part of the early-deposited mineral phase of bone [43] and even on the surface of nanocrystalline synthetic HA [44] has suggested that the so-called precursors may be just the detectable part of a newly forming poorly crystalline apatite of reduced dimensions [45].

The controversy of the in vivo process can help to understand certain aspects in the formation of nano-apatite coatings issued of deposition methods close to physiological conditions such as ECAD. Particularly, in the present in vitro approach we have detected a slight splitting in the v_4 phosphate region for some spectra of so-called "transitional ACP" (Fig. 7). According to Rey et al. [30], a more detailed spectral analysis in that region could be useful to elucidate if, what has been considered as ACP in this study, corresponds instead to a non apatitic disordered domain present at the outermost surface of poorly crystalline and highly hydrated nucleating apatite. The underlying crystalline domains would only become detectable once they acquire enough surface-to-volume ratios as compared to the interfacial non-apatitic phase. The HA nanocrystals on the surface of transient spherical ACP nanoparticles detected by Rössler et al. [26] by means of highly magnified SEM could be ascribed instead to newly nucleating crystalline domains at the highly hydrated surface domains of apatitic cores rather than ACP spheres.

While more detailed studies are needed to fully understand the mechanisms of apatite formation, ECAD system is a successful method to produce collagen–hydroxyapatite substrates similar to biological bone besides orientation of the deposited crystals. GlcA, in turn, has demonstrated to be a successful molecule to advance deposition of highly crystalline HA when bound to collagenous substrates. The similarities found in the early CPP formation for ECAD and Simulated Body Fluid (SBF) [46], suggest that the advance in CPP deposition promoted by GlcA-modified collagen substrates would also take place in the case of SBF exposure. The lower relative supersaturating conditions at the surface of the substrates subjected to SBF would probably lead to a delayed deposition in time as compared to ECAD. Although less suitable for producing implant coatings, the slower SBF-mediated mineralization may help to obtain additional information on the process of apatite formation.

4.3 Influence of pS on the mineralization of pure collagenous substrates

Phosphoproteins such as OPN and BSP are also part of the ECM of bone and are discussed as mediators of the in vivo biomineralization [9–11, 22–24]. Phosphoserine (pS) was chosen as a model for this group of biomolecules and added to the electrolyte in order to observe its potential inhibitory effect on the process of crystallization. Thus pS serves as an example for the way in which soluble additives act in the natural process in opposition to the promotion of mineralization they show when present in immobilized form [47–50].

In the presence of pS the formation of crystalline HA is retarded above molar ratios for pS/Ca^{2+} of 1:200. This

indicates that pS in the electrolyte serves as an inhibitor of crystallization of HA. For the highest applied concentration, pS also acts as a mineralization inhibitor because the amount of deposited CPP is clearly diminished as it has been detected by electron microscopy mapping and by the decrease in the intensity of the FTIR signals.

The model for CPP nucleation on titanium substrates proposed by Rössler et al. [26], together with the assumption that pS forms calcium-containing complexes would explain why less homogeneous coatings are obtained with increasing amounts of pS in the electrolyte. In the proposed model the nuclei formed in the electrolyte would either reach the surface and nucleate or re-dissolve again. This latter situation would be favored by the formation of Ca–pS complexes in the electrolyte, resulting in less CPP on the surface due to a shift of the deposition/redissolution equilibrium towards increased redissolution.

Morphologically, the shape of the coatings formed varies with the increasing pS concentration in the electrolyte. This variation consists in the progressive agglomeration of the phosphate phases obtained. Our explanation is based on the known fact that pS is able to form complexes with Ca^{2+} ions [22–24, 51–53]. Thus in solutions with higher concentration ratios of pS/Ca^{2+}, Ca^{2+} will be increasingly bound by the increasing concentration of pS molecules present via the two anionic functionalities (phosphate and carboxylate). On the one hand this will impede the interaction of Ca^{2+} with inorganic phosphate ions, reducing the amount of deposited CPP. On the other hand the complex will give rise to agglomerates, as pS molecules may also bridge different Ca^{2+} ions. The resulting topography gives for intermediate concentrations of pS an amalgam of amorphous and crystalline elements (Figs. 8e, 9b2, 9b3) changing into a supra-aggregation of non-crystalline calcium phosphates (Figs. 8h, 9c3) for even higher concentrations.

4.4 Mineralization of GlcA–collagen substrates in the presence of pS containing electrolytes

The simultaneous influence of the two model molecules studied in this work, GlcA immobilized on the collagenous substrate and pS present in solution, on the crystallization behaviour is GlcA/pS dose-dependent. The formation of the thermodynamically stable mineralization product HA, which is promoted by GlcA in absence of pS, clearly does not occur in presence of a 1:40 pS/Ca^{2+} ratio (Fig. 8c, f). In analogy to the effect on unmodified matrices, pS probably achieves retardation of the process by attracting Ca^{2+} that could otherwise be bound by the GlcA modified collagen substrates.

Concerning the morphology of CPP phases on GlcA-modified matrices for 30 min of deposition, on the 1:40 pS/Ca^{2+} ratio samples we find again an aggregated structure (Fig. 8i). In the competition for Ca^{2+}, the pS influence may possibly dominate over GlcA due to the concentration used, the higher number of functionalities of the first [51] and the immobilized state of the second. The ability of Ca^{2+} to bridge the existing anionic functionalities from GlcA and pS (one per GlcA molecule and two per pS molecule) may be the reason for this similar effect of aggregation [52], yet the binding of Ca^{2+} to anionic groups is usually cooperative and involves at least two or three ligands [53].

5 Summary

Model molecules carrying functional groups, which are known to play an important role in biomineralization, can be used for influencing the mineralization behavior and the morphology of the resultant Calcium Phosphate Phases in vitro, either singly or in combination. Thus, this model-based approach has proven useful to provide new insights in these complex processes, circumventing the myriad of interactions happening in the real framework in which these molecules are present in nature. Both models are certainly not able to map completely PGs or Phosphoprotein resulting properties in their structures but, alternatively, these simple formulations become an asset for the novel design of implant coatings, which may allow stimulating the peri-implant mineralization process with lower immunogenic risk as compared to the use of complete biological molecules.

Additional experiments will help to understand more precisely the mechanisms governing the interactions between the molecules studied, and possibly allow the generation of more bone-like substrates. Interestingly, the application of this strategy is already suitable to produce bioactive implant coatings and may result in an improved healing, though this is still to be determined by means of further testing.

Acknowledgements The authors thank: Sophie Rössler, Thomas Hanke and Klaus Becker for their technical assistance and helpful discussions.

References

1. De Jonge LT, Leeuwenburgh SCG, Wolke JGC, Jansen JA. Organic–inorganic surface modifications for titanium implant surfaces. Pharm Res. 2008;25(10):2357–69.
2. Rössler S, Born R, Scharnweber D, Worch H, Sewing A, Dard M. Biomimetic coatings functionalized with adhesion peptides for dental implants. J Mater Sci Mater Med. 2001;12:871–7.
3. Bierbaum S, Douglas T, Hanke T, Scharnweber D, Tippelt S, Monsees T, et al. Collageneous matrix coatings on titanium

implants modified with decorin and chondroitin sulfate: characterization and influence on osteoblastic cells. J Biomed Mater Res A. 2006;77:551–62.
4. Morra M. Biochemical modification of titanium surfaces: peptides and ECM proteins. Eur Cell Mater. 2006;12:1–15.
5. Jäger I, Fratzl P. Mineralized collagen fibrils: a mechanical model with a staggered arrangement of mineral particles. Biophys J. 2000;79(4):1737–46.
6. Mann S. Biomineralization. Principles and concepts in bioinorganic materials chemistry. Oxford University Press; 2001.
7. Boskey AL. Matrix proteins and mineralization: an overview. Connect Tissue Res. 1996;35:357–63.
8. Schliephake H, Scharnweber D, Rössler S, Dard M, Sewing A, Aref A. Biomimetic calcium phosphate composite coating of dental implants. Int J Oral Maxillofac Implants. 2006;21:738–46.
9. Wuttke M, Müller S, Nitsche DP, Paulsson M, Hanisch FG, Maurer P. Structural characterization of human recombinant and bone-derived bone sialoprotein. Functional implications for cell attachment and hydroxyapatite binding. J Biol Chem. 2001;276: 36839–48.
10. Hunter GK, Goldberg HA. Modulation of crystal formation by bone phosphoproteins: role of glutamic acid-rich sequences in the nucleation of hydroxyapatite by bone sialoprotein. Biochem J. 1994;302:175–9.
11. Hunter GK, Kyle CL, Goldberg HA. Modulation of crystal formation by bone phosphoproteins: structural specificity of the osteopontin-mediated inhibition of hydroxyapatite formation. Biochem J. 1994;300:723–8.
12. Paschalakis P, Vynios DH, Tsiganos CP, Dalas E, Maniatis C, Koutsoukos PG. Effect of proteoglycans on hydroxyapatite growth in vitro: the role of hyaluronan. Biochim Biophys Acta. 1993;1158:129–36.
13. Waddington RJ, Hall RC, Embery G, Lloyd DM. Changing profiles of proteoglycans in the transition of predentine to dentine. Matrix Biol. 2003;22:153–61.
14. Paschalakis P, Vynios DH, Tsiganos CP, Koutsoukos PG. Inhibition of hydroxyapatite in vitro by glucosaminoglycans: the effect of size, sulphation and primary structure, in water soluble polymers, solution properties and applications. In: Amjad Z ed. New York: Plenum Press; 1998. P. 63–75.
15. Iozzo RV. The biology of the small leucine-rich proteoglycans. Functional network of interactive proteins. J Biol Chem. 1999;274:18843–6.
16. Keene DR, Antonio JDS, Mayne R, McQuillan DJ, Sarris G, Santoro SA, et al. Decorin binds near the C terminus of type I collagen. J Biol Chem. 2000;275:21801–4.
17. Hunter GK, Poitras MS, Underhill TM, Grynpas MD, Goldberg HA. Induction of collagen mineralization by a bone sialoprotein-decorin chimeric protein. J Biomed Mater Res. 2001;55:496–502.
18. Goldoni S, Owens RT, McQuillan DJ, Shriver Z, Sasisekharan R, Birk DE, et al. Biologically active decorin is a monomer in solution. J Biol Chem. 2004;279:6606–12.
19. Ding A, Ojingwa JC, McDonagh AF, Burlingame AL, Benet LZ. Evidence for covalent binding of acyl glucuronides to serum albumin via an imine mechanism as revealed by tandem mass spectrometry. Proc Natl Acad Sci. 1993;90:3797–801.
20. Casu B. Structural features and binding properties of chondroitin sulfates, dermatan sulfate, and heparan sulfate. Semin Thromb Hemost, Istituto di Chimica e Biochimica G. Ronzoni, Milan, Italy. 1991;17:9–14.
21. Vogel KG, Trotter JA. The effect of proteoglycans on the morphology of collagen fibrils formed in vitro. Coll Relat Res. 1987;7:105–14.
22. Aoba T, Moreno EC. Adsorption of phosphoserine onto hydroxyapatite and its inhibitory activity on crystal growth. J Colloid Interface Sci. 1985;106:110–21.
23. Misra DN. Interaction of ortho-phospho-l-serine with hydroxyapatite: formation of a surface complex. J Colloid Interface Sci. 1997;194:249–55.
24. Reinstorf A, Ruhnow M, Gelinsky M, Pompe W, Hempel U, Wenzel KW, et al. Phosphoserine - a convenient compound for modification of calcium phosphate bone cement collagen composites. J Mater Sci Mater Med. 2004;15:451–5.
25. Leon B, Jansen JA. Thin calcium phosphate coatings for medical implants. Springer; 2008.
26. Rössler S, Sewing A, Stölzel M, Born R, Scharnweber D, Dard M, et al. Electrochemically assisted deposition of thin calcium phosphate coatings at near-physiological pH and temperature. J Biomed Mater Res A. 2003;64:655–63.
27. Sewing A, Lakatos M, Scharnweber D, Rössler S, Born R, Dard M, et al. Influence of Ca/P ratio on electrochemical assisted deposition of HAP on titanium. Key Eng Mater. 2004;254–256:419–22.
28. Lowry O, Rosebrough NJ, Farr AL, Randall RJ. Protein measurement with the Folin phenol reagent. J Biol Chem. 1951; 193:265–75.
29. Mecozzi M, Dragone P, Amici M, Pietrantonio E. Ultrasound assisted extraction and determination of the carbohydrate fraction in marine sediments. Org Geochem. 2000;31:1797–803.
30. Rey C, Combes C, Drouet C, Lebugle A, Sfihi H, Barroug A. Nanocrystalline apatites in biological systems: characterization, structure and properties. Mat-wiss u Werkstofftech. 2007;38(12): 996–1002.
31. Koutsopoulos S. Synthesis and characterization of hydroxyapatite crystals: a review study on the analytical methods. J Biomed Mater Res. 2002;62:600–12.
32. Combes C, Rey C, Mounic S. Identification and evaluation of HPO_4 ions in biomimetic poorly crystalline apatite and bone mineral. Key Eng Mater. 2001;192–5:143–6.
33. Birk DE, Lande MA. Corneal and scleral collagen fiber formation in vitro. Biochim Biophys Acta. 1981;670:362–9.
34. Iberg N, Flückiger R. Nonenzymatic glycosylation of albumin in vivo. Identification of multiple glycosylated sites. J Biol Chem. 1986;261:13542–5.
35. Garlick R, Mazer J. The principal site of nonenzymatic glycosylation of human serum albumin in vivo. J Biol Chem. 1983; 258:6142–6.
36. Born R, Scharnweber D, Rössler S, Stölzel M, Thieme M, Wolf C, et al. Surface analysis of titanium based biomaterials. Fresenius J anal Chem. 1998;361:697–700.
37. Elliot JC. Structure and chemistry of the apatites and other calcium orthophosphates. 2nd ed. Amsterdam: Elsevier; 1994. p 58–60, 259–63.
38. Posner A, Blumethal NC, Betts F. Chemistry and structure of precipitated hydroxyapatites. In: Nriagu JO, Moore PB, editors. Phosphate minerals. Berlin/Heidelberg: Springer Verlag; 1984. p. 155–71.
39. Lowenstam HA, Weiner S. On biomineralization. New York: Oxford University Press; 1989.
40. Crane NJ, Popescu V, Morris MD, Steenhuis P, Ignelzi MA Jr. Raman spectroscopic evidence for octacalcium phosphate and other transient mineral species deposited during intramembranous mineralization. Bone. 2006;39:434–42.
41. Weiner S. Transient precursor strategy in mineral formation of bone. Bone. 2006;39:431–3.
42. Mahamid J, Sharir A, Addadi L, Weiner S. Amorphous calcium phosphate is a major component of the forming fin bones of zebrafish: indications for an amorphous precursor phase. Proc Natl Acad Sci USA. 2008;105:12748–53.
43. Rey C, Simizu M, Collins B, Glimcher MJ. Resolution-enhanced Fourier transform infrared spectroscopy study for the environment of phosphate ion in the early deposits of a solid phase of

calcium phosphate in bone and enamel and their evolution with age: 2. Investigations in the v_3 PO_4 domain. Calcif Tissue Int. 1991;49:383–8.
44. Jäger C, Welzel T, Meyer-Zaika W, Epple M. A solid-state NMR investigation of the structure of nanocrystalline hydroxyapatite. Magn Reson Chem. 2006;44:573–80.
45. Grynpas MD. Transient precursor strategy or very small biological apatite crystals? Bone. 2007;41:162–4.
46. Scharnweber D, Born R, Flade K, Rössler S, Stölzel M, Worch H. Mineralization behaviour of collagen type I immobilized on different substrates. Biomaterials. 2004;25:2371–80.
47. Linde A, Lussi A, Crenshaw MA. Mineral induction by immobilized polyanionic proteins. Calcif Tissue Int. 1989;44:286–95.
48. Addadi L, Weiner S. Interactions between acidic proteins and crystals: stereochemical requirements in biomineralization. Proc Natl Acad Sci USA. 1985;82:4110–4.
49. Addadi L, Moradian J, Shay E, Maroudas NG, Weiner S. A chemical model for the cooperation of sulfates and carboxylates in calcite crystal nucleation: relevance to biomineralization. Proc Natl Acad Sci USA. 1987;82:2732–6.
50. Van den Bos T, Beertsen WJ. Bound phosphoproteins enhance mineralization of alkaline phosphatase-collagen complexes in vivo. Bone Miner Res. 1994;9:1205–9.
51. Glimcher MJ. Mechanism of calcification: role of collagen fibrils and collagen-phosphoprotein complexes in vitro and in vivo. Anat Rec. 1989;224:139–53.
52. Benaziz L, Barroug A, Legrouri A, Rey C, Lebugle A. Adsorption of o-phospho-l-serine and l-serine onto poorly crystalline apatite. J Colloid Interface Sci. 2001;238:48–53.
53. Glimcher MJ. Disorders of bone and mineral metabolism. In: Fredric LC, Murray JF, editors. New York: Raven Press; 1992. P. 26.